Influence of long time ageing on ductility and toughness in the stainless steel 310 in the presence of banded microstructure

M. Farooq, R. Sandström

During service at elevated temperatures extensive formation of particles can take place that can have a dramatic influence on mechanical properties. Precipitation of σ-phase and $M_{23}C_6$-carbides have been studied both experimentally and with thermodynamic modelling for 25Cr20Ni austenitic stainless steels (AISI 310) at 800 ºC for up to 5000 h. Previous work has demonstrated that the modelling could describe the nucleation and growth satisfactory. After long term ageing the particles form bands in the microstructure. In the present paper the influence of these bands on ductility and toughness at room temperature is analysed. For this purpose previously developed models for ductility and toughness are utilised. Model values for banded and non-banded microstructures have been generated for casts of 310 in fine and coarse grained conditions with 0.04 and 0.12%N. The model values show that in the coarse grained condition, no reduction in ductility and toughness can be expected in the banded microstructure. In the fine grained condition a modest reduction is predicted.

Keywords:
austenitic stainless, long time ageing, elevated temperature, precipitation, ductility, toughness

INTRODUCTION

Segregation is the non-uniformity of chemical elements between parent liquid and solidified cast product of steel. Segregation is aligned into longitudinal bands by hot rolling called banding. The banding affects the mechanical properties of steel.

Grange [1] studied the effect of microstructural banding in low alloy steels. Microstructural banding caused anisotropy in mechanical properties. He found that banding reduced tensile ductility and toughness of steel with lowered the shelf energy. Banding had also some effect on strength. In normalized steel or annealed banded hypoeutectoidic steels, low variations on transversal and longitudinal tensile properties can be found and significant variation of both reduction in area and impact properties can be observed [2].

The presence of microstructural bands in AL-6XN, a commercial super-austenitic stainless steel, has been examined [3]. It was found that the microstructural bands have elevated levels of chromium and molybdenum and decreased level of nickel and iron. σ-phase was the prominent phase within bands. The presence of brittle sigma particles within the bands can cause crack initiation and a continuous band of large precipitates reduces the ductility of steel. In [4] the corrosion and microstructural anomalies of fractured high nitrogen stainless steel femoral component were investigated. They found that regions of banding and grains near the surface were present on both the failed and retrieved Exeter stems. Briant and Hall [5] observed that the amount of corrosion in low carbon AISI 316 steel increased with increase in carbide precipitation. Compositional banding also increased the amount of corrosion.

Muhammad Farooq, Rolf Sandström
Materials Science and Engineering, KTH,
Brinellv. 23, 100 44 Stockholm, Sweden

Paper presented at the 7th European Stainless Steel Conference - Como, 21-23 September 2011, organized by AIM

The research work in the present paper is a continuation of two previous articles by the authors [6], [7], where particle formation in the austenitic stainless steel 310 were quantified. In particular σ-phase and $M_{23}C_6$-carbides were analysed. Specimens were aged up to 5000 h at 800 ºC. The precipitation of the two phases were modelled. The basis of the model was diffusion controlled growth. σ-phase showed spherical growth and $M_{23}C_6$ planar growth. The soft impingement of the diffusion zones with respect to both chromium and carbon was taken into account. The sizes and the volume fractions were successfully predicted.

Ageing in general first increased the strength due to precipitation of fine $M_{23}C_6$. This effect was gradually reduced due to the growth of the carbides. The strength was also influenced by reduced solid solution hardening due to alloy element depletion. A model was developed for the influence of ageing on the ductility. The model takes into account how the stress distribution around particles changes the uniform elongation. Chen and Knott's model for the influence of coarse particles on fracture toughness was further developed and used successfully.

The purpose of the present paper is to characterise and quantify the precipitation across the bands of streaks in the microstructure of austenitic stainless steel 310 during long time aging and their effect on mechanical properties.

MATERIAL AND EXPERIMENTAL DETAILS

The material used in the present investigation was an AISI 310 austenitic stainless steel. Its composition is 25%Cr 20%Ni 0.05%C. For details about composition, production and heat treatment of material, see [6]. Four different heats: low N fine grained, low N coarse grained, high N fine grained and high N coarse grained were investigated for ageing times up 5000 h at 800 ºC. These heats were studied by light optical microscopy (LOM), scanning electron microscopy (SEM) and wavelength dispersive spectroscopy (WDS). The EDS spot analysis and WDS were used to identify the particles.

PREDICTIONS WITH THERMO-CALC

Thermo-Calc has been used to calculate the amount of different phases as a function of temperatures [8]. Thermo-Calc database TCFE4 has been applied. The phase fractions for the high N material are shown in Fig. 1 and those of high N material with higher Cr and C in Fig. 2.

The main phase is σ-phase in Fig. 1. About 1% of $M_{23}C_6$ exists below 900 ºC. Comparing Figs. 1 and 2, it can be seen that the mole fraction of $M_{23}C_6$ carbide in Fig. 2 is much higher than in Fig. 1. When Cr and C composition increases, then the amount of carbide $M_{23}C_6$ increases. The equilibrium amount of σ-phase in Fig. 2 at 800 ºC is about 5% whereas it is 2% in Fig. 1.

The composition of the equilibrium phases according to Thermo-Calc is given in Table 1. $M_{23}C_6$ contains Cr, C and some Fe contents. The main elements in σ-phase are Cr and Fe and some Ni.

MODELLING OF PRECIPITATION

Nucleation

The nucleation of precipitates is generally modelled with the help of classical nucleation theory. The nucleation rate N_r can be determined as [6]

$$\frac{dN_r}{dt} = \frac{D_{Fe} N_v}{a_0^2} \exp\left(-\frac{G^*}{kT}\right) \quad (1)$$

where D_{Fe} is the self diffusion coefficient, a_0 the atomic spacing, G* the Gibbs energy barrier to nucleation, N_v the number of potential nucleation sites at grain boundaries or grain corners per unit volume, k Boltzmann's constant and T the temperature in Kelvin.

Growth

Quasi-stationary models based on control by volume diffusion have been used to determine the velocity for planar and spherical growth of the nuclei [6]. The resulting models are

$$\frac{dr}{dt} = \frac{D_{Cr}}{r} \frac{\Omega^2}{2(1-\Omega)} \left(1 - \frac{1}{\Omega_2} \frac{r}{r_{lim}}\right) \quad \text{(Planar growth)} \quad (2)$$

$$\frac{dr}{dt} = \frac{D_{Cr}}{r} \frac{Z(\Omega)\Omega}{2(Z(\Omega)-1)} \left(1 - \frac{1}{\Omega_2} \frac{r^3}{r_{lim}^3}\right) \quad \text{(Spherical growth)} \quad (3)$$

where

$$Z(\Omega) = \frac{\sqrt{\Omega^2 + 8\Omega} - \Omega}{2\Omega}$$

$$\Omega = \frac{x_{Cr}^{\gamma} - x_{Cr}^{\gamma/\sigma}}{x_{Cr}^{\sigma/\gamma} - x_{Cr}^{\gamma/\sigma}} \quad (4)$$

r is in the case of planar growth half the thickness of the grain boundary film or radius of the nucleus for spherical growth and t the time. D_{Cr} is the diffusion coefficient for the controlling element, in this case chromium since its diffusion is slower than for iron and nickel. The supersaturation of the controlling alloying element (Cr) is referred to as Ω. X_{Cr}^{γ} is the Cr content of the steel (in mol) with its matrix γ-phase. $x_{Cr}^{\gamma\sigma}$ is the Cr content of γ in equilibrium with the precipitate in this case σ. $x_{Cr}^{\sigma/\gamma}$ is the Cr content of the precipitate in equilibrium with γ.

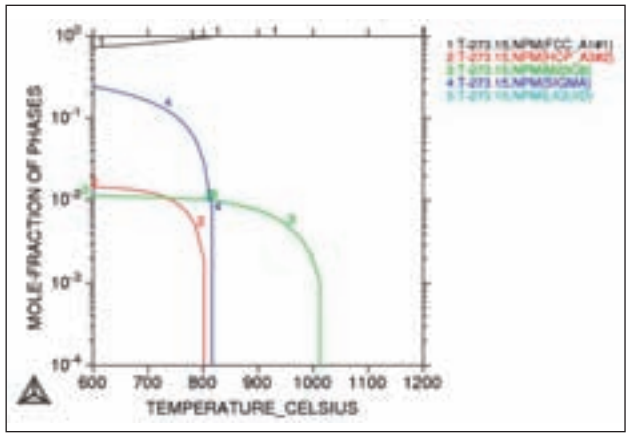

FIG. 1 ***Equilibrium phase fractions for 310 0.12N.***

Frazioni di fasi all'equilibrio per l'acciaio 310 0.12N.

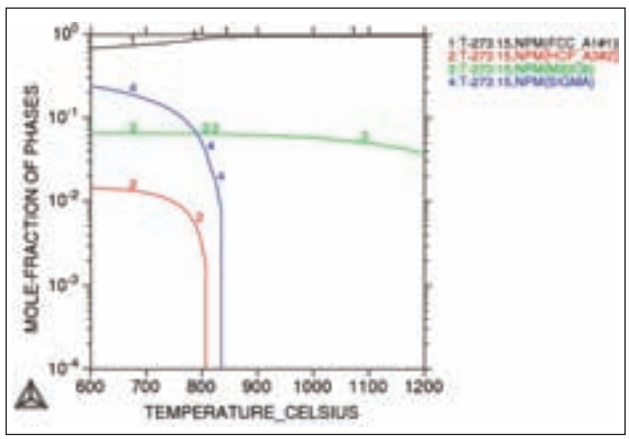

FIG. 2 ***Equilibrium phase fractions for 310 0.12N with 28%Cr and 0.3%C.***

Frazioni di fasi all'equilibrio per l'acciaio 310 0.12N con 28%Cr e 0.3%C

Interparticle distance

When modelling ductility and toughness, the distance between neighbouring coarse particles play an important role. These coarse particles consist mainly of σ-phase. The nucleation and growth of σ-phase take place normally at the grain boundaries. In that case the average interparticle distance d_{part} can be estimated to

$$d_{part} = 2a\sqrt{\frac{\pi a}{D_{grain} f_{vol}}} \quad (5)$$

Cast	Phase	Vol. fract., mol	Si	Cr	Fe	Ni	Mn	N	C
0.036N	$M_{23}C_6$	0.009	0	82.2	10.9	0.8	0.4	0	5.6
0.036N	σ	0.072	0.5	46.3	47.2	5.8	0.3	0	0
0.12	$M_{23}C_6$	0.010	0	82.2	11.0	0.8	0.4	0	5.6
0.12	σ	0.029	0.4	46.2	47.3	5.8	0.3	0	0
0.12	Cr2N	0.005	0	88.0	0.8	0.1	0.1	10.6	0.5

Tab. 1 ***Compositions of equilibrium phases according to Thermo-Calc at 800 ºC, wt%.***

Composizione delle fasi all'equilibrio secondo Thermo-Calc a 800 ºC, peso%.

where a is particle radius, D_{grain} the grain size, and f_{vol} the volume faction of particles. However, when bands are formed, the coarse particles are no longer located at the grain boundaries, but rather homogeneously distributed in the matrix. In that case the interparticle distance is given by

$$d_{part} = 2a \cdot \sqrt{\frac{\pi}{6 f_{vol}}} \quad (6)$$

OBSERVED PRECIPITATION

Wavelength dispersive spectroscopy

Streaks of particles have been observed. To identify these particles, their composition has been determined with the help of wavelength dispersive spectroscopy (WDS). A streak of particles is shown in Fig. 3. The particle marked 1 contains chromium and iron to about 40% and nickel to 15%. This particle is σ-phase. From the composition of particle marked 2 it can be concluded that it is a $M_{23}C_6$ carbide. Evidently streaks may consist of both types of particles.

Scanning electron microscopy

The particle structure after aging 2000h at 800 ºC is also analysed by scanning electron microscopy (SEM) in Fig. 4. The particles have been identified with the help of EDS spot analysis. In Fig. 4 particles are marked with numbers. Particles 1 & 3 have chromium, carbon and iron contents of 75%, 4%, 13% respectively. These particles are $M_{23}C_6$ carbides. Particle 2 has about 40% chromium and iron contents. This particle is σ-phase.
In Fig. 5 a band of the particles is shown. The variation of chemical composition along a line across the band has been measured by Line SEM as shown in Fig. 6. The average value of Cr and C across the band has been determined to 28% and 0.3% respectively. Area fraction of particles across band has been measured to 14% using image J software. This is the highest volume fraction found.

Light optical metallography

Light optical pictures of specimens of the high N, coarse grained heat, aged for 500, 2000, 5000 h have been recorded. σ-phase is observed at the grain boundaries. At the two longer ageing times, finer 23-carbides are easily seen at the grain boun-

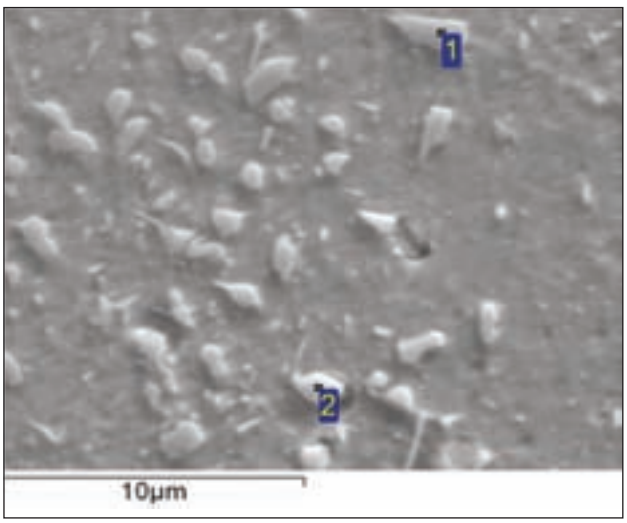

FIG. 3 ***WDS image of high N cast, coarse grained and aged for 2000 h at 800 ºC.***

Immagine WDS di getto con alto tenore di N, con grani grossi e invecchiato per 2000 h a 800 ºC.

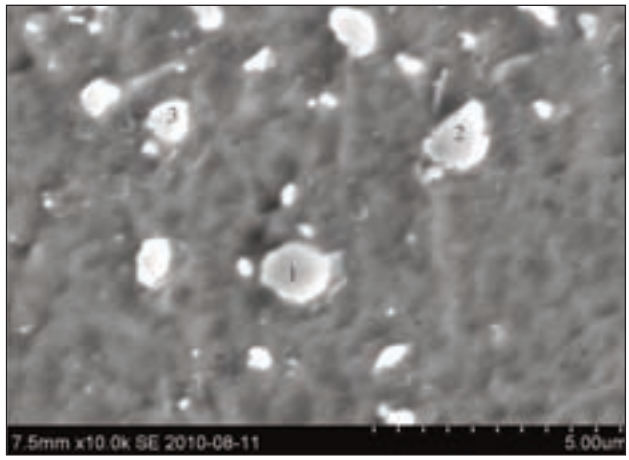

FIG. 4 ***SEM image of High N cast, coarse grained and aged for 2000h at 800 ºC.***

Immagine SEM di getto con alto tenore di N, con grani grossi e invecchiato per 2000 h a 800 ºC.

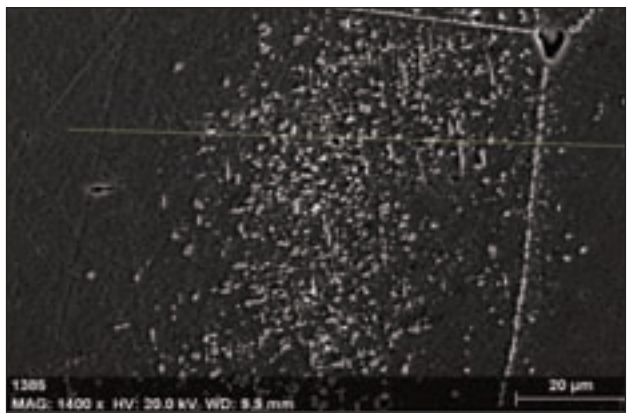

FIG. 5 ***Line SEM image of high N cast, coarse grained and aged for 2000h at 800 ºC.***

Immagine SEM con linea di riferimento di un getto con alto tenore di N, avente grani grossi e invecchiato per 2000 h a 800 ºC

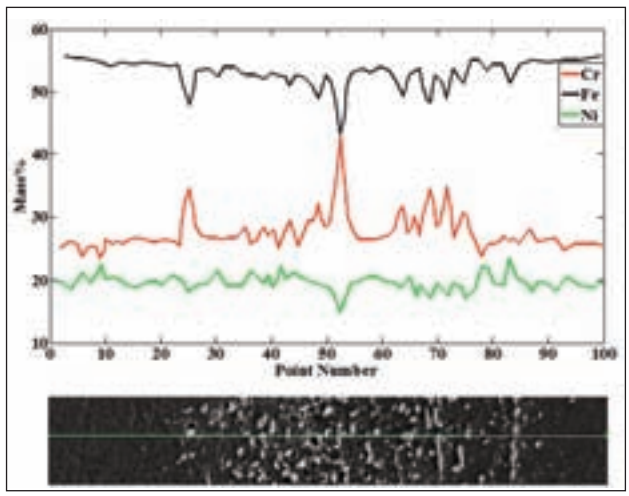

FIG. 6 ***Variation of compositions across band for SEM image of High N cast, coarse grained and aged for 2000h at 800 ºC.***

Variazione nella composizione attraverso la banda nell'immagine SEM, per il getto con alto tenore di N, con grani grossi e invecchiato per 2000 h a 800 ºC.

daries. With increasing aging time both type of particles increase and grow. In the low N heats a banded microstructure with streaks is also present.
In the corresponding micrographs for the low N cast, the amount of σ-phase is clearly much higher than for the high N cast. Also lower amounts of 23-carbides are precipitated for the high N cast than for the low N cast. The same applies to the streaks. Some coarsening of 23-carbides in the streaks is clearly observed, but the size of the carbides is not very large.
In Fig. 7 micrograph for the fine grained high N heat aged 5000h is shown. If the microstructures are compared to the corresponding coarse grained heat, the σ-phase is considerably larger in the fine grained heat and the precipitation of $M_{23}C_6$ is quite extensive in the fine grained heat, but is hardly observable in the coarse grained heat.
For the low N fine grained heat, the growth of the σ-phase during ageing is evident. Carbides are also observed at slip bands. These crabides also change in size with ageing time.

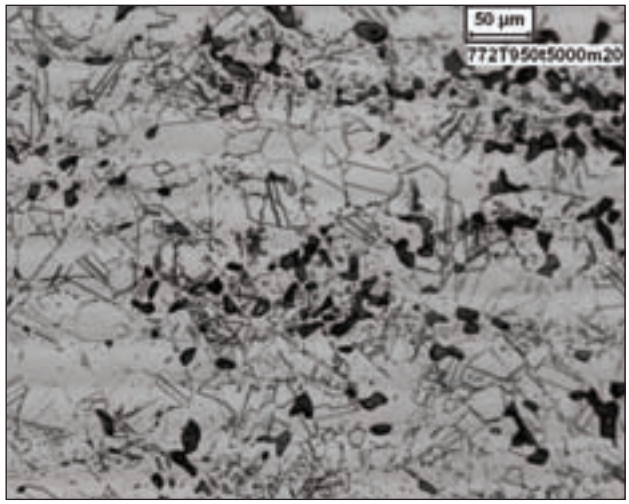

FIG. 7 ***Light optical micrographs for the high N cast, fine grained, aged 5000 h.***
Micrografia ottica del getto con alto tenore di N, con grani fini, invecchiato per 5000 h.

DUCTILITY

The limit of the forming capability of a material is controlled by plastic instability. When this instability is reached a crack is rapidly formed and failure occurs. In a tensile test the plastic instability is associated with the uniform elongation and the failure with the total elongation. The ductility decreases with increasing aging time and volume fraction of σ for all casts.
To model the ductility, the stress strain curves must be known. For austenitic stainless steels the stress strain curves can many times be represented by the Kocks-Mecking relation

$$\sigma = A - Be^{(-\omega\varepsilon)} \tag{7}$$

A, B and ω are constants, σ the stress and ε the strain. A is approximately the (true) tensile strength and A-B the yield strength. There are stress concentrations around larger particles, such as σ-phase located at grain corners. The critical position for the plastic instability is then between particles at grain edges perpendicular to the loading direction. Along such an edge the stress is given by

$$\sigma_{conc} = \sigma_{appl} + \frac{1}{2}\left(1 - \frac{E_{part}}{E_{matr}}\right)\sigma_{appl}\left(\frac{a^2}{r^2} + \frac{3a^4}{r^4}\right) \tag{8}$$

σ_{appl} is the applied stress, and E_{part} and E_{matr} are the elastic modulus in the particle and the matrix, respectively. a is the radius of the particles and r is the distance from the centre of a particle. The average value along an edge represents the critical stress level

$$\sigma_{ave} = \frac{1}{d_{grain}/2 - a}\int_a^{d_{grain}/2} \sigma_{conc}\, dr \tag{9}$$

When Considère's criterion is fulfilled, plastic collapse takes place. This occurs when the uniform elongation ε_u is reached. Solving the equation for Considère's criterion gives

$$\varepsilon_u = -\frac{1}{\omega}\ln\left(\frac{A}{B}\left(1 - \frac{\omega\sigma_{appl}}{(\omega+1)\sigma_{ave}}\right)\right) \tag{10}$$

Further details of the model can be found in [7]. Eq. (10) is compared to experimental data in Fig. 8. For the homogeneous (non-banded) structure the interparticle distance according to eq. (5) has been used, for the banded structure eq. (6). The nucleation and growth of particles are described by eqs. (1) to (4).
From Fig. 8 it is evident that the banding does not automatically reduce the ductility. Only for the fine grained cast there can be a reduction if the volume fraction of particles is high in the bands. This can be understood in the following way. In the non-banded microstructure the coarse particles are located at the grain boundaries which gives a small distance between particles. However, for the banded structure the particles are mainly found in the grain interiors, and this gives a larger interparticle distance, in particular for the coarse grained casts.

TOUGHNESS

A model due to Chen and Knott [9] has been used. The basic assumption in this model is that failure takes place when the distance between cracked particles is less than the critical crack opening displacement (COD). The fracture toughness K_c is given by

$$K_c = \varepsilon_u\sqrt{\frac{2\pi(1+\nu)\sigma_{gy}\sigma_y d_{part}}{5a}} \tag{11}$$

ε_u is the uniform elongation, ν Poisson's number, σ_{gy} stress for general yield, σ_y yield strength, d_{part} average distance between cracked particles, and a particle radius.
Predicted fracture toughness values according to (11) are compared to experimental data in Fig. 9. In the same way as for the ductility, the interparticle distance is determined with eqs. (5) and (6) for homogeneous and banded microstructure, respectively.
The models of the fracture toughness for the banded and non-banded microstructure are not very different for the fine grained casts. For the coarse grained cast the model for the banded structure gives results that are above those of the non-banded structure. Thus, even if the high volume fraction of particles in the bands is taken into account the reduction in toughness is modest.

CONCLUSIONS

Ageing of austenitic stainless steel 310 at 800 ºC generates a significant amounts of precipitation in the form of σ-phase and carbides $M_{23}C_6$. The modelling of nucleation and growth of these particles has successfully been accomplished in previous work. Coarse σ-phase particles are found at grain boundaries and intragranularly in bands. These coarse particles influence the ductility and toughness. Models for this influence has previously been derived. In the present paper these models are used to describe the role of particles in bands.
Long term ageing of 310 gives rise to bands in the microstructure where the volume fractions of particles is much higher than in the remainder of the matrix. Volume fractions of up to 14% has been recorded.

FIG. 8

Uniform elongation as a function of volume fraction of σ-phase. Model values for non-banded (homogeneous) and banded microstructures are compared to experimental data for type 310 aged at different times at 800 ºC; a) fine grained 310 with 0.04N; b) coarse grained 310 with 0.04N; c) fine grained 310 with 0.12N; d) coarse grained 310 with 0.12N.

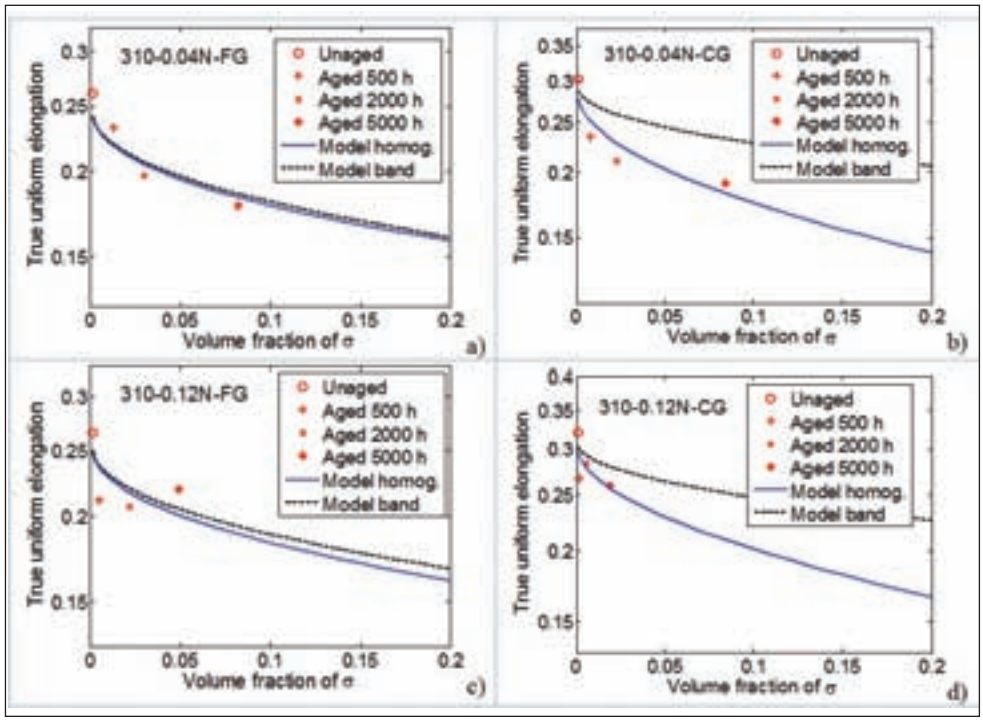

Allungamento uniforme in funzione della frazione di volume della fase . Valori modello per microstrutture senza bande (omogenee) e con bande sono confrontati con dati sperimentali per l'acciaio 310 invecchiato per tempi diversi a 800 ºC; a) acciaio 310 a grano fine con 0.04N; b) acciaio 310 a grano grosso con 0.04N; c) acciaio 310 a grano fine con 0.12N; d) acciaio 310 a grano grosso con 0.12N.

FIG. 9

Fracture toughness as a function of volume fraction of σ-phase. Model values for non-banded (homogeneous) and banded microstructures are compared to experimental data for type 310 aged at different times at 800 ºC; a) fine grained 310 with 0.04N; b) coarse grained 310 with 0.04N; c) fine grained 310 with 0.12N; d) coarse grained 310 with 0.12N.

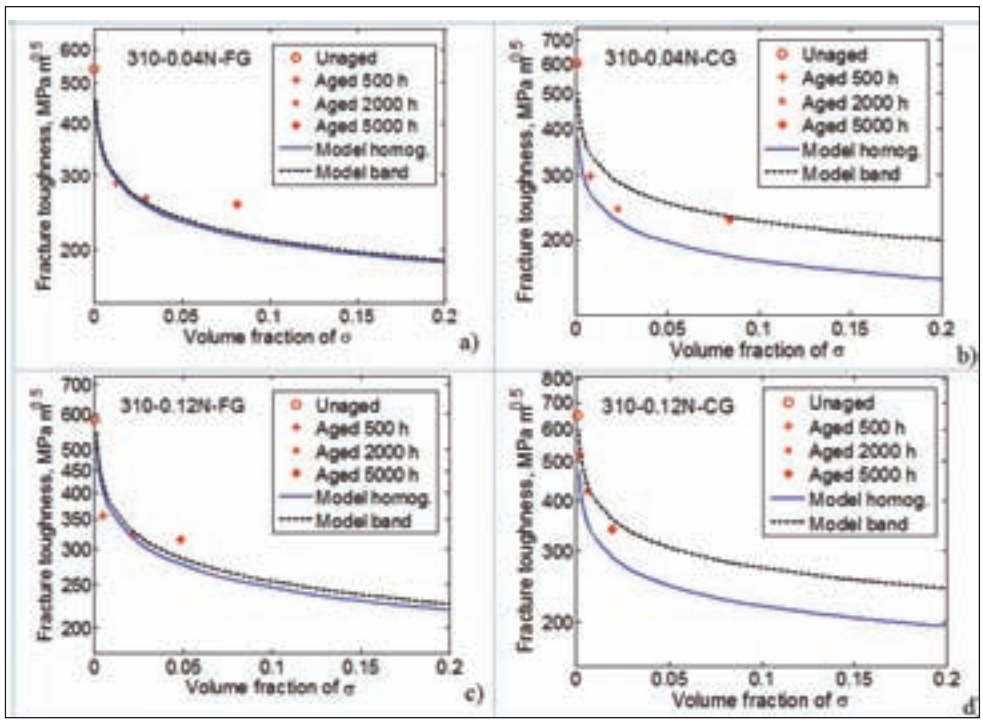

Resistenza alla frattura in funzione della frazione di volume della fase . Valori modello per microstrutture senza bande (omogenee) e con bande sono stati confrontati con dati sperimentali per l'acciaio 310 invecchiato per tempi diversi a 800 ºC; a) acciaio 310 a grano fine con 0.04N; b) acciaio 310 a grano grosso con 0.04N; c) acciaio 310 a grano fine con 0.12N; d) acciaio 310 a grano grosso con 0.12N.

- The particles across the band are mostly $M_{23}C_6$ carbides, but σ phase is also found. The amount of banding increases with increasing ageing times.
- The coarse σ-phase particles that are expected to influence ductility and toughness are initially mainly located at grain boundaries but later also in bands.
- In the models for both ductility and toughness, the interparticle distance play an important role. Different expressions have been used for the interparticle distance for banded and non-banded microstructure.

- Both for ductility and toughness the models values are somewhat lower for the banded than for the non-banded microstructure for the fine grained casts considering high volume fraction of σ. However, for coarse grained casts this is not the case. The model values are in reasonable agreement with the measured mechanical properties.

ACKNOWLEDGEMENTS
Financial support from the Consortium for Materials Science in Thermal Energy Processes (project KME-402), Outokumpu Stainless and Sandvik Materials Technology is gratefully acknowledged. The authors would like to thank Bo Ivarsson and Mats Lundberg from these two companies for supplying material and data.

REFERENCES

[1] R.A. GRANGE, Metall. Trans. 2, (1971), p.417.
[2] J. FAIL, ANAL and PREVEN, Springer 10, (2010), p.351.
[3] A.C. STAUFFER, D.A. KOSS and J.B. MCKIRGAN, Metall. Materials Trans A 35, (2004), p.1317.
[4] E. SWARTS, A. KOP, S. MILLER and C. KEOGH, Transactions 7th world biomaterials congress, (2004), p.494.
[5] C.L. BRIANT and E.L. HALL , Corrosion 43, (1987), p.525.
[6] R. SANDSTRÖM, M. FAROOQ and M. LUNDBERG, Precipitation during long time ageing in the austenitic stainless steel 310, subm. for publ. 2011.
[7] M. FAROOQ, R. SANDSTRÖM and B. IVARSSON, Influence of particle formation during long time ageing on mechanical properties in the austenitic stainless steel 31, subm. for publ. 2011.
[8] B. SUNDMAN, B. JANSSON and J. O. ANDERSSON, The Thermo-Calc Databank System, Calphad 9, (1985), p.153.
[9] C.Q. CHEN and J.F. KNOTT, Met. Sci.e, 15, (1981), p.357.

Abstract

Influenza dell'invecchiamento prolungato su duttilità e tenacità nell'acciaio inox 310 in presenza di microstruttura a bande

Parole chiave: acciaio inossidabile – invecchiamento - modellazione

Durante il servizio a temperature elevate si può verificare una considerevole formazione di particelle che possono avere un'influenza radicale sulle proprietà meccaniche. Nel presente lavoro precipitazione di fase σ e dei carburi $M_{23}C_6$ sono stati studiati sia sperimentalmente che mediante modellazione termodinamica per gli acciai inossidabili austenitici 25Cr20Ni (AISI 310) a 800 °C per un massimo di 5000 h. Lavori precedenti hanno dimostrato che la modellazione potrebbe descrivere la nucleazione e la crescita in modo soddisfacente. Dopo un invecchiamento prolungato le particelle formano bande nella microstruttura. Nel presente lavoro viene analizzata l'influenza di queste bande sulla duttilità e tenacità a temperatura ambiente. A tale scopo sono stati utilizzati i modelli precedentemente sviluppati per la duttilità e la tenacità. Sono stati generati valori di modello per microstrutture con bande e senza bande per getti di acciaio 310 in situazioni di grana fine e grana grossa, con 0,04 e 0,12% N. I valori del modello mostrano che in condizioni di materiali a grana grossa, non si prevede alcuna riduzione di duttilità e tenacità nel caso di microstruttura a bande. In materiali a grana fine è prevista una modesta riduzione.